## Session 2A (4) – Phased Array Applications

*Chairman* – ***Prof B Drinkwater***

**16.15** **The application of Phased Array Ultrasonic Techniques for inspection of railway axles from their end face**

*Authors* - ***Dimosthenis Liaptsis, John Jian, Kevin Boyle, Miles Weston, P. Ian Nicholson, Joana A Courinha and Mr Pedro Barros, Margarida Pinto***

*The structural integrity of wheel sets used in rolling stock is of great importance to the rail industry and its customers. A number of rail accidents have been directly related to the failure of wheels and axles, leading to increased demands for the inspection and maintenance of such components. This paper presents the initial study of the development of a phased array ultrasonic inspection system for inspection of railway axles and details the inspection of the axles from their end face. The advantage of inspecting from the end face is the ability to deploy the phased array technique in situ without the need to fully disassemble the wheel sets. End face inspections are presented including different pulse echo and pitch-catch techniques. Results are presented and compared with a series of modelling studies undertaken using CIVA ultrasonic modelling software. The ultrasonic simulation results have shown a good agreement with the experimental results obtained during this study.*

# The application of phased array ultrasonic techniques for inspection of railway axles from their end face

Dimosthenis Liaptsis, Ian Cooper, John Jian,
Kevin Boyle, Miles Weston, P Ian Nicholson
TWI NDT Validation Centre (Wales),
Port Talbot, SA13 2EZ, UK
Tel: +44 (0)1639 873100
Fax: +44 (0)1639 864679
E-mail: dimos.liaptsis@twi.co.uk

Joana A Courinha, Pedro Barros, Margarida Pinto
Instituto de Soldadura e Qualidade (ISQ),
2740-120 Porto Salvo, Portugal

**Abstract**

As part of the development of a new manual Non Destructive Testing (NDT) system combining complementary inspection techniques, an inspection system based on Phased Array Ultrasonic Testing (PAUT) for detection of transverse cracking in solid railway axles is being developed. This paper presents the initial study, which includes the PAUT experimental setup and the initial results obtained after testing the system on railway axle test blocks. In this study the inspection of solid axles from their axle end face is investigated. The goal to performing the inspections from the axle end face is the advantage that the wheelset can be inspected whilst still on the train and therefore with minimal wheelset disassembly. Different end face inspection scanning configurations are presented including pulse echo and pitch-catch techniques. The experimental results are compared to assess the probe's detection capabilities and to determine the sensitivity that can be achieved. Experimental results show that spark eroded notches of depth 1mm, 3mm and 5mm introduced on the wheel seat and on adjacent curved areas of the axle test blocks were all detectable from the axle end face. In addition to practical experimentation, a series of modelling studies were undertaken using CIVA ultrasonic modelling software, to simulate the wave propagation and the interaction of ultrasound with the introduced flaws in the axle blocks.

## 1. Introduction

SAFERAIL[(1)] is a collaboration between EU companies and research organisations supporting the effort of the rail industry in achieving better safety standards by developing new methodologies and techniques for the inspection of wheelsets. Both wheels and axles are safety critical components and appropriate inspection techniques are being investigated under the SAFERAIL project. As part of the development of a new manual Non Destrucitve Testing (NDT) system combining complementary inspection techniques for inspection of wheelsets, a Phased Array Ultrasonic Testing (PAUT) System is being developed. This paper presents work carried out specifically targeting the inspection of rail axles. The authors have already reported PAUT for the inspection of solid axles using probes positioned on the axle wheel seats [(2)]. However, although this method of inspection is acceptable for scheduled major overhaul periods when worn wheels are removed and there is therefore good access to the wheel seat surface, this inspection regime could be disruptive and costly to train operating companies if carried out on a more frequent basis.

The risk of axle failure relates to both mileage and time. Therefore, it is better if more frequently scheduled inspections occur during the lifetime of the axle rather than waiting for the less frequent overhaul periods in order to detect any growing fatigue cracks. Indeed, strict rail standards throughout Europe exist to ensure that axles are inspected at regular and frequent periods to ensure safety is maintained. To be cost effective and to cause minimal disruption to train services, the NDT inspection should not require the disassembly of the wheel sets and supporting bogies.

In this study, the inspection of solid axles from their end face is investigated. The main objectives of the work presented in this paper are to determine the factors affecting the detectability of the introduced transverse notches in axle test blocks and determine the most suitable inspection parameters to inspect the axle from the end face.

In addition to practical experimentation, a series of modelling studies were undertaken to simulate the wave propagation and the interaction of ultrasound with the introduced flaws in the axle using CIVA[(3)] ultrasonic modelling software. The analysis of the beam propagation and interaction with the defects have been simulated in order to optimize and predict the performance of the phased array experiments in real train wheelsets. Several possible probe orientations and defect locations have been simulated. The different configurations result in different capabilities of detection, which helped guide the experimental procedure.

## 2. Experimental approach

### *2.1 Axle Test blocks*

The development work included the design and manufacture of two axle test blocks. After feedback from the SAFERAIL end user partners, machined transverse flaws with a range of different sizes were implanted in critical locations on the axle blocks. Test blocks were manufactured from a single axle, cut into three sections to allow greater manoeuvrability and handling of the parts. Cuts were made using a mechanical saw that produced an accurate geometric finish. In test block 1, three Electrical discharge machining (EDM) surface breaking notches were machined into the surface of the wheel seat, equidistance around its circumference. Figure 1 shows the detailed Computer Aided Design (CAD) drawing of test block 1, where three surface breaking notches were introduced at the wheel seat region. In test block 2, three EDM notches were introduced into both curved surfaces adjacent to the wheel seat, equidistance around the circumference. Notches in the R75 region were offset from notches in the R51 region by an angle of 30º to minimise the chance of interference during inspection. All the machined notches have a circumferential length of 25mm and a varying depth from the axle surface of 5mm, 3mm and 1mm. The width of the notches is 0.3mm. Each critical region has three notches of different depths.

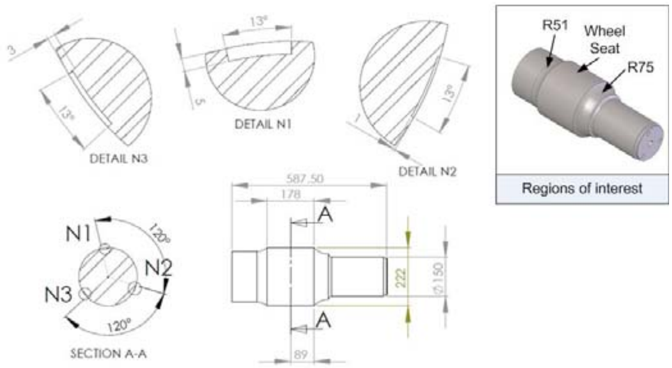


**Figure 1. CAD drawing of test block 1 showing details of the machined EDM notches**

## *2.2 Experimental set up*

The system used to inspect the test blocks comprised a Micropulse 5PA 128/128 channel array controller, manufactured by PeakNDT [4]. An Olympus, R/D Tech, 1-D linear 64 element probe was used for the pulse echo investigations and two GE 32 element probes were used in the pitch-catch investigations. The probes were placed in direct contact with the test block end faces for the initial technique development. The software platform used to acquire the ultrasonic data and drive the array controller, was ArrayGen, developed by PeakNDT. Figure 2 shows the equipment and one test block used to obtain the phased array data presented in this report.

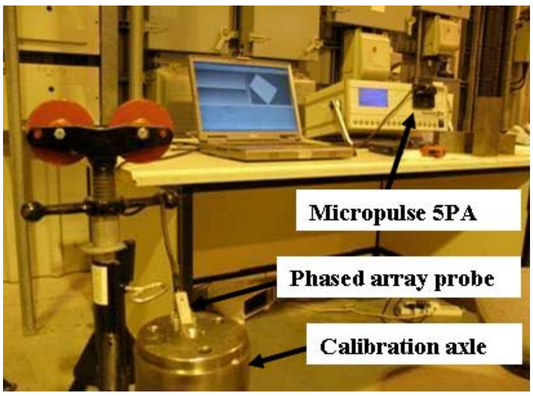


**Figure 2. Experimental set up and apparatus used to inspect the test axle blocks**

### *2.2.1 Phased array inspection from the axle end face*

Figure 3 shows the different probe configurations trialled on the test axles blocks in order to cover specific regions of the axle. Figure 3a shows the position of the phased array probe on the test axle 1 to inspect the EDM notches introduced into the wheel seat. Similarly, Figures 3b and 3c show the probe position on test axle block 2 to inspect the curvatures on the R75 and R51 regions, respectively. The probes were scanned around the surface of the axle test block end face and the response from each of the notches was monitored and recorded using the Micropulse equipment. To identify the machined notches from the geometrical features of the axle, both the sectorial scan and A-scan data sets were used. This data combination assists the identification and sizing of the machined EDM notches.

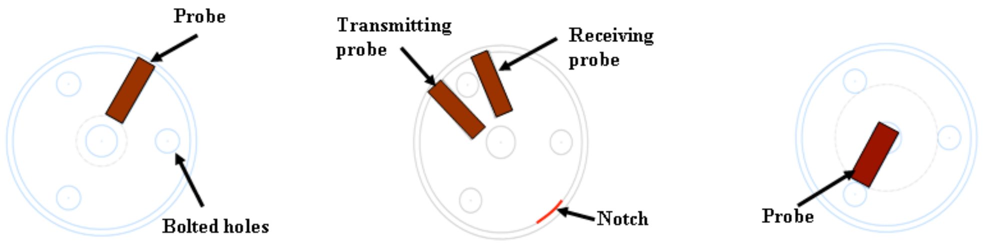


**Figure 3. Inspection configurations from the end face (a) pulse echo from outer part (b) pitch-catch from outer part (c) pulse echo from inner part**

The parameters used to obtain the phased array data from the axle test samples presented in the paper are shown in Table 1.

**Table 1. Experimental parameters used for the data acquisition**

| Parameters for Olympus probe | Parameters for GE probe |
|---|---|
| Probe: 5L-64-A2<br>No. Elements: 64<br>Element pitch: 0.6mm<br>Aperture used: 64 elements<br>Centre Frequency: 5MHz<br>Wave Type: Longitudinal<br>Scan Type: Sectorial<br>Sweep Angle Range: 0º to 60º<br>Angle Resolution: 0.5º<br>Focal Depth: 222mm | Probe: 115 000 189<br>No. Elements: 32<br>Element pitch: 1mm<br>Aperture used: 32 elements for pitch-catch from outer part and 16 elements for pulse-echo from inner part<br>Centre Frequency: 5MHz<br>Wave Type: Longitudinal<br>Scan Type: Sectorial<br>Sweep Angle Range: 0º to 60º<br>Angle Resolution: 0.5º<br>Focal Depth: 222mm |

## 3. Experimental results and discussion

### *3.1 Inspection from the end face outer part using the pulse-echo method*

*3.1.1 Inspection of the wheel-seat region*

Inspection of the wheel seat region was carried out using the probe configuration shown in Figure 3a and the inspection parameters presented in Table 1 for the 64 elements Olympus probe. Sectorial and A-Scan images were obtained for all the notches in test block 1 using the setup described above. By applying a gate on the A-Scan display, the material longitudinal velocity could be determined to be within ±2m/s. The longitudinal velocity for the axle material was found to be 5,900m/s. Figure 4a presents the optimum incident angle that was used for the inspection of the wheel seat region. Figure 4 also presents the sectorial phased array data from a non-defective region of the wheel-seat and where there is the presence of the introduced transverse EDM notches (5mm, 3mm and 1mm). It can be seen that, in the absence of defects in the wheel-seat region, the only reflection is due to the corner of R51 curvature region B. It is important to identify reflections caused due to axle geometrical features in order to avoid false calls.

In the presence of transverse defects at the wheel-seat region a reflection occurs at the corner of the EDM notch and, therefore, it was possible to detect the introduced EDM notches. By controlling the gain within the software a high Signal to Noise Ratio (SNR) was achieved. However, it is more difficult to identify the tip diffraction echo from the notches that will assist in the accurate sizing of the notches. The tip diffraction has a weak echo due to the small reflected amplitude coming from the tip, and also the reflected ultrasonic wave is scattered at different directions to the incidence direction. These two factors contribute to the weak response received from the notch tip. Another difficulty encountered in identifying the tip echo is the distance that the ultrasonic wave needs to propagate through the material. The further the beam travels the higher is the material attenuation, as well as the beam spread. As the ultrasonic beam diverts due to the beam spread and, consequently, the beam width becomes wider, this in turn reduces the inspection resolution and reduced reflected amplitude from the defects. All the aforementioned factors contribute to the difficulty in distinguishing between the corner echo and the tip diffraction. From this set of experiments, it was shown that it is possible to detect the notches introduced at the wheel-seat region when the phased array probe is placed at the outer surface of the axle end face.

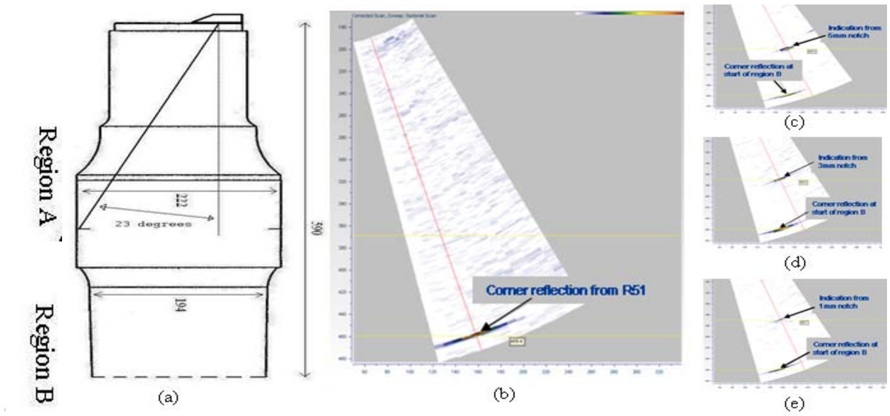


**Figure 4. Inspection of the wheel-seat region (a) optimum inspection angle (b) sectorial view from an axle area without defect present (c) data from 5mm notch (d) data from 3mm notch (e) data from 1mm notch**

*3.1.2 Inspection of the R75 curvature region*

The spark eroded notches in R75 curvature region A could not be detected in this trial when the probe was positioned on the outer part of the end face as shown in Figure 3a. Attempts were made to direct a sound beam straight onto the notch, and also to skip off the axle's side wall onto the notch, but neither technique was successful. The reasons that a sound beam could not be directed normal to the notch interface are: (1) lack of access at the end face due to the presence of three holes; (2) notch orientation relative to the ultrasonic beam direction and (3) combination of both.

3.1.3 *Inspection of the R51 curvature region*

In the presence of defects at the R51 curvature region B a reflection occurs at the corner of the EDM notch and, therefore, it was possible to detect the introduced EDM notches at the R51 curvature region B. Figure 5 shown the optimum ultrasonic incidence angle used to test the R51 curvature for the detection of the transverse EDM notches and the A-scan response and the sectorial data from a 1mm notch. As mentioned previously, it is not possible to accurate size the defects since it is difficult to detect a reflection from the defect tip due to the weak response.

From this set of experiments, it was shown that it is possible to detect all the notches introduced at the R51 curvature region B when the phased array probe is placed at the outer surface of the axle end face despite the presence of the bolted holes used to attach the bearing cap.

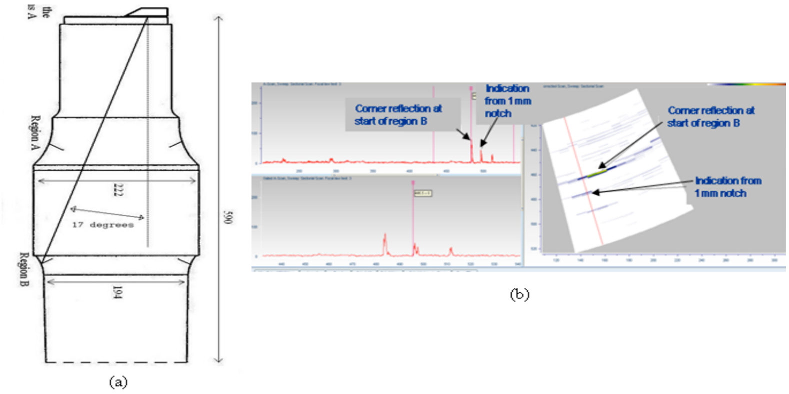


**Figure 5. Inspection of the R51 curvature region A (a) optimum inspection angle (b) A-scan and sectorial scan from the 1mm EDM notch**

### *3.2 Inspection of R75 curvature region A from the end face outer part using the pitch-catch method*

Section 3.1.2 explained that when the probe was positioned on the outer part of the end face and the pulse-echo method employed, it was not possible to detect the introduced notches in the R75 curvature region. Therefore, a pitch-catch technique was investigated. Two GE probes with the parameters presented in table 1 were used. Using the pitch-catch technique and with the probes positioned as shown in Figure 3b it was possible to detect the notches in the R75 curvature region A with a probe placed either side of the botl hole cavity. Figure 6 shows that using the pitch-catch technique it is possible to detect the 1mm notch. The the lack of access due to the presence of the threaded holes was overcome by using the pitch-catch method

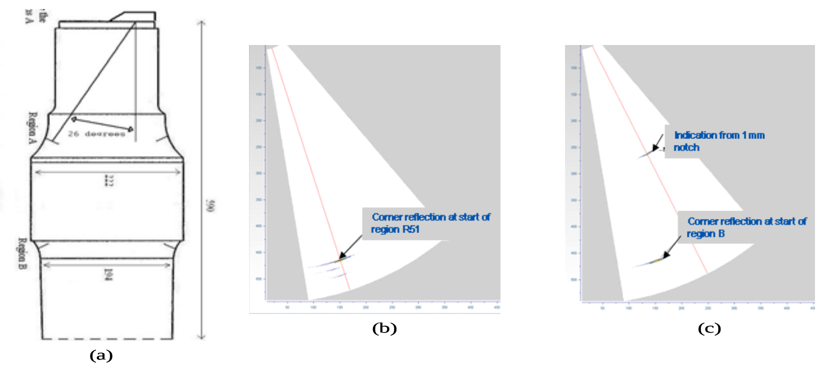


**Figure 6. Inspection of the R75 region A using pitch catch (a) optimum inspection angle (b) sectorial view from an axle area without defect present (c) data from 1mm notch**

### *3.3 Inspection from the axle end face inner part using the pulse-echo method*

This trial was carried out to investigate the possibility of detecting spark eroded notches in a railway axle when transmitting phased array ultrasound through the inner part of the axle end face (see Figure 3c). It should be noted that, although the same GE 5MHz phased array probe was used for these trials, only 16 of the 32 available elements were used. This reduced the active aperture of the probe so that the active area of the probe was coupled to the shaft between the threaded hole and the centre spigot hole, as shown in Figure 3c. All the notches in all three different areas of interest have been detected using this approach. Figure 7 shows the phased array data from the 1mm notches introduced in the wheel-seat, R75 and R51 curvature, respectively. The optimum detection incidence angles are: 21º for wheel-seat, 24º for R75 curvature and 16º for R51 curvature.

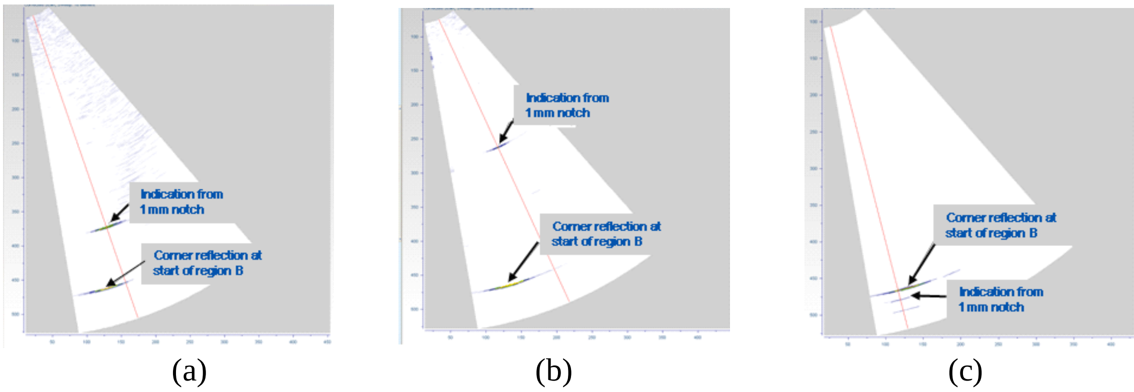


**Figure 7. Sectorial data obtained using pulse-echo from inner part of end face from the 1mm notches at (a) wheel-seat (b) R75 curvature (c) R51 curvature**

## 4. Ultrasonic modelling results

### *4.1 Approach*

In addition to the practical trials, a series of ongoing modelling experiments have been performed using CIVA ultrasonic modeling software, version 9.1a, in order to aid future development. The beam characteristics and capability of flaw detection are being studied by simulating acoustic pressure distribution and amplitude of response.

### *4.2 Experimental parameters and procedure*

The geometry of the test blocks was reproduced in a CAD environment, due to its complex shape. This 2D configuration was afterwards introduced in CIVA, where the 3D configuration took place.

In this task, the train axle geometry was tested in the area shown in Figure 8 (the wheel-seat area). The notch configurations were reproduced in the CIVA environment, in accordance with the geometrical information detailed in section 2.1. A set of three surface breaking notches with a length of 25mm and depths of 5mm, 3mm and 1mm from the axle surface were defined and located in each of the two positions of interest.

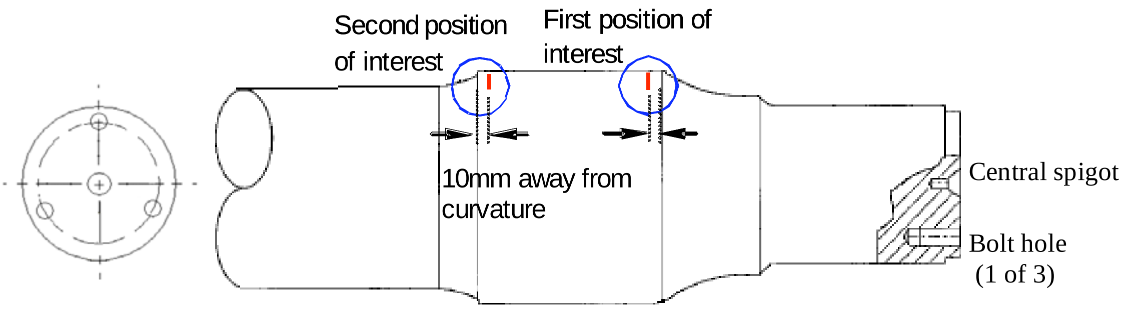


**Figure 8. Identification of the inspected areas**

The probes being investigated were built in CIVA according to the parameters presented in table 1. In order to compare and to determine the effect of different frequency and bigger element pitch an additional probe was modelled for pulse echo inspection. This additional probe has 60 elements with a centre frequency of 7.5MHz and an element pitch of 1mm. The modelling was conducted for a number of different configurations including different probes and different wedges. The modelling reported here presents the investigative work towards the optimised conditions and as such, two types of wedges are included in the simulation. The wedges are currently in manufacture and future experimental work will be carried out to confirm the modelling results.

Figure 9 illustrates the probes position and the inspection configurations used in the modelling. As the end face is being used for probe placement, it was necessary to consider the bolt hole cavities in the surface (Figure 8). Since sound cannot be propagated through the cavities, this places a limitation on the probe placement and possible beam angle. Figure 9a shows the general configuration of the probe position on the end face, considering this limitation. Due to the depth of these cavities inside the axle, and the angle range performed in the simulations, the probe aperture had to be reduced (no total aperture was used) to avoid beam interference with the cavities' edges. The simulations were carried out in a sectorial scan with multipoint focusing. The focal points were placed along a specific area around the notch positions in the surface of the specimen. This ensured the area near the surface was always covered by the beam focus.

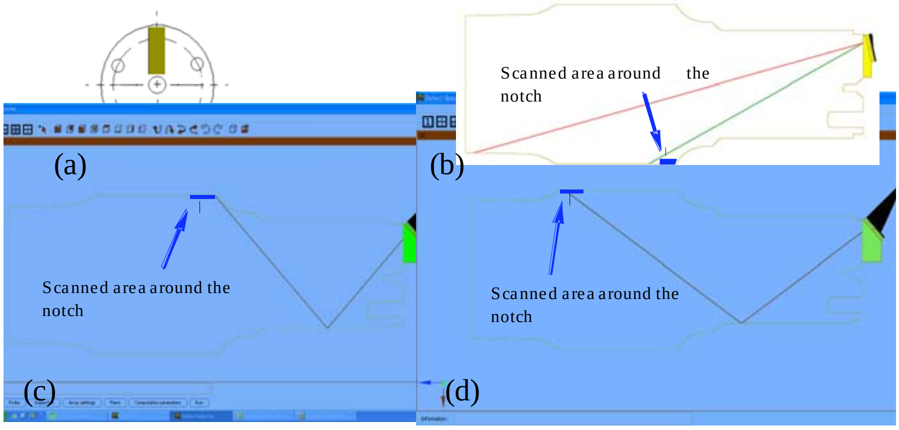


**Figure 9. Configuration of the modeling (a) Probe position on end face (b) Direct incidence, first area of interest (c) Indirect incidence, second area of interest (d) Indirect incidence, second area of interest**

For the simulations, the probe remained in a fixed position which was at the same location for all the probes. The interaction with the notches was made by electronic scan. The probe does not need to be physically displaced in its active axis because the beam angle can be altered electronically and therefore achieve good coverage from a single probe position. The procedure followed for these simulations included three investigations.

For the initial investigation, the 64 element 5MHz probe was configured with the parameters defined previously and in addition a 30º wedge was included, as shown in Figure 9b. A 0º wedge was not used to access this area, due to strong beam deflection. In order to avoid the interference of the beam with the curved surface of the R75, and the consequent beam spread, the aperture had to be reduced to 19 elements.
The first position of interest in the wheel-seat area was then scanned, with a direct incidence of the beam, in a beam computation mode, in order to determine beam shape. In this approach, it was not possible to obtain incidence angles above the first critical angle. Therefore, longitudinal waves have been modelled. For this investigation, a sweep angle range of 28º to 30º was used. It should be noted that the steep angle used in the modelling differs from the experiments which did not use wedges. This is because of the different position of the notches modelled in the wheel-seat area.
The second investigation involved modelling the same region (the wheel-seat area), but with an indirect incidence of the beam, using backwall reflection, as represented in Figure 9c. For this purpose a 55º wedge was added to both 5MHz and 7.5MHz probes. The incident angles were more favorable than with the first investigation, and above the first critical angle, so shear waves were modelled. Due to the presence of the bolt holes in the axle the number of active elements was reduced to 50 for the 5MHz probe, and to 30 for the 7.5MHz probe, to avoid interference with the holes. The defect response was simulated for both 5MHz and 7.5MHz probes. The aim was to perform a new beam computation, to visualize beam shape, to simulate the interaction with the EDM notches, and to identify the best probe that accessed the area of interest.
The third investigation involved modelling the probe previously selected (7.5MHz) to access the second area of interest, again through the backwall reflection. The same parameters as in the previous investigation were used. Due to the new angle range, the aperture was set to 48 elements.

### *4.3 Ultrasonic modelling results and discussion*

From the simulations performed, two set of results are shown in Figure 10 using the 64 elements 5MHz probe parameters. The first image represents an overlay of the notch reflection and a 3mm side drilled hole (SDH) reflection placed in the same position as the notch, acting as a reference reflector. The second image illustrates the distribution of acoustic pressure around the notch, with the reflections from the surface and the tip.
In CIVA the A-scan alone does not give enough information since it is not displayed in a scale of absolute decibels. Instead, it comes in a relative scale that does not allow the capability of detection to be determined without comparing a response from a flaw to another reference response. For this reason, a simulation with a SDH was performed along with every notch simulation, in order that all the reflections from the notches could be compared to a fixed reference. This allowed easier comparison of the results from the different probes.
Depending on notch detectability in a certain modelling configuration, the response obtained from the notch presents a certain amplitude drop (or dB drop) from the SDH

reference response. The dB drops for all the notches were determined relative to the respective SDH, as represented in Figure 10a.

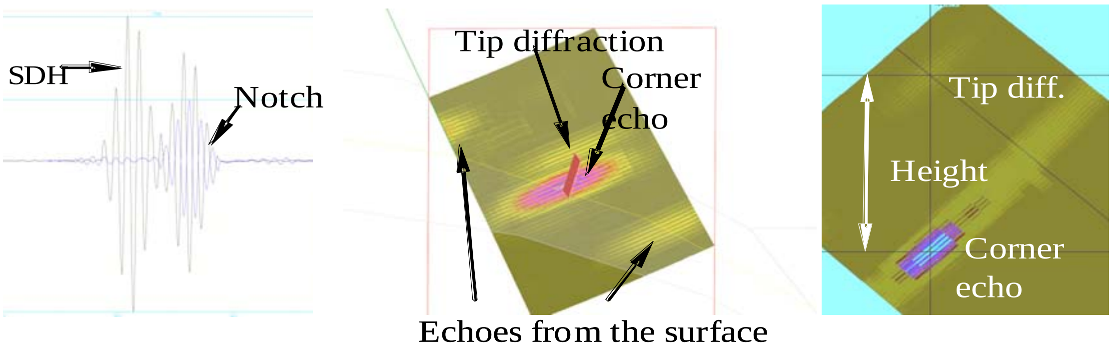


(a) (b) (c)

**Figure 10. Examples of CIVA results: (a) A-scan (b) Acoustic pressure distribution (c) Dimensioning environment**

For the beam computations in the first investigation the direct incidence showed that the beam is easily intercepted by the geometry of the R75 curvature, spreading out before reaching the area of interest (Figure 11a). Only a small aperture can avoid this interference, with the drawback of a very short focal range. In the example of Figure 5b 19 active elements were used, and the probe does not have enough focal range to access the area of interest (the depth of the field is within -10dB). Therefore, this approach was abandoned.

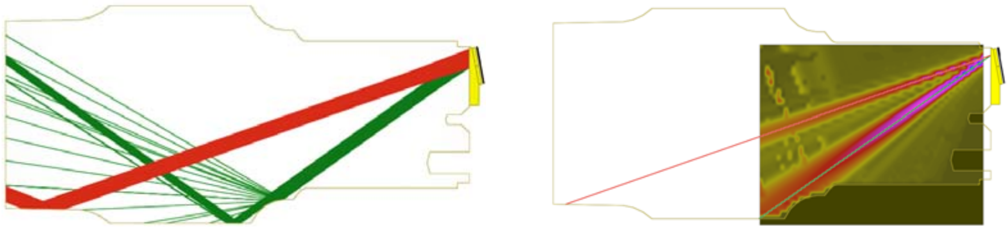

(a) (b)

**Figure 11. First area of incidence, 5MHz Olympus 5L-64 probe, direct incidence. (a) 32 active elements – interference of the beam with the surface (b) 19 active elements – extremely short focal range**

For the second and third investigations, the results showed that all notches were detectable and their responses were compared with the responses from the SDHs, in order to ascertain the dB drop from the reference reflector. The simulated results showed that there was a dB increase compared to the reflection from a 3mm SDH of 16dB, 14dB and 7dB for the 5mm, 3mm and 1mm notches, respectively. The modelling has shown it is possible to detect and separate the corner echo and the tip diffraction only for the 5mm and the 3mm notches, which allows for the dimensioning of their heights. The 5MHz probe can insonify the first area of interest keeping the depth of the field within -3dB. Even though the modelled 5MHz probe results show that the probe has enough focal range to access this area, the 7.5MHz probe has a longer near field region. In fact, as can be seen in figure 12, even with only 30 active elements, the

7.5MHz probe can reach the firs area of interest keeping the depth of the field within -1.5dB and therefore it was chosen for accessing the second area of interest. These simulation results will be verified experimentally in future work.

(a) (b)

**Figure 11. Focal range in the first area of interest.**
**Indirect incidence (a) 5MHz (b) 7.5MHz**

## 5. Conclusions

This paper has demonstrated that it is possible to detect the nine spark eroded notches in the axle using the equipment listed and using a combination of pulse-echo and pitch-catch phased array inspection techniques applied from the axle end face. It should be noted that the threaded blind holes in the end face of the axle create potential blind spots for all three regions when using pulse-echo, and that to ensure that one scan gives 100% coverage of each region it may be necessary to use a bank of probes and a multigroup system. It should also be noted that although the EDM notches have been detected using the configurations described, it was not possible to accurately size them. This is due to the use of longitudinal waves that have longer wavelength and beam spread.
It is possible to detect the nine spark eroded notches located within the three regions from the inner scan path using the equipment listed. Although inspecting the axle from the inner scan path can be achieved with one phased array probe, and without the need for multi probes, it should be noted that the resulting scans were noisier in the first 50mm distance from the endface. This is most likely due to the probe being closer to the centre spigot hole.
The modelling has shown that all the notches placed in the wheel-seat region could be detected using the backwall reflection. It is conclusive from the ultrasonic modelling beam computation results that the acoustic pressure is stronger for the 7.5 MHz probe, making it a better choice for this application, even with less active elements than in the 5MHz probe. From the results it is evident that a direct incidence of the beam in the notches, placed in the first position of interest, is not a good option, since the beam is intercepted by the geometry of the R75 curvature, causing it to spread and miss part of the area near the notch position. The ultrasonic modelling results and conclusions will be verified experimentally by carrying out inspections with shear waves and using both the 64 elements 5MHz probe and the 60 elements 7.5MHz probe that was modelled.
An indirect incidence, using the backwall reflection, allows for more favorable angles of incidence in the notch (around 45º), which intensify corner effect, revealing a much stronger and more reliable interaction that comply with a better detectability. Along with this advantage, there is the elimination of the longitudinal wave, avoiding the existence of more than one propagation mode.

All the notches, including the 1mm height, were clearly detected, giving and amplitude of response above the SDH reflection, both in the nearest and the farthest positions of interest. In terms of notch height, the 5mm and the 3mm notches could be dimensioned, which gives more confidence to the results.
Inspecting from the axle end face using PAUT has been shown to be a promising technique. The advantage of the inspection of axles from their end face is the ability to deploy the phased array technique in situ without the need to disassemble the wheelset and thus reduce the train wagon downtime. The only disassembly required for this inspection technique would be the removal of the end cap from each axle end. One possible limitation is different axle types. Some axle types have different hole size and depth cavities present at the end face. Depending on the size, these holes can limit the probe placement since sound cannot be propagated through them.
The laboratory conditions are very different to the real axle environment. Therefore further work through testing of real axles is required in order to determine if when performing the inspections insitu, the flaw indications can be diststinguished from indications not only due to axle geometry but also due to echos from any attached break disk, bearings, sealing rings and wheel and bogey structures.

**Acknowledgements**

SAFERAIL is collaboration between the following organisations: Alfa Products & Technologies, EMEF SA, Envirocoustics A.B.E.E., Feldman Enterprises LTD, Instituto de Soldadura e Qualidade, Société Nationale des Chemins de fer Français (SNCF), Technical Software Consultants Ltd, TWI Ltd, University of Birmingham, Vlaamse Vervoersmaatschappij De Lijn, VTG Rail UK Ltd. The authors are particularly grateful to the end users, VTG Rail UK Ltd and EMEF SA, for the provision of samples.
The research leading to these results has received funding from the European Community's Seventh Framework Programme (FP7/2007-2013) under grant agreement n° 218674.

**References**

1. http://www.saferail.net [accessed 18th August 2010]
2. D Liaptsis, P Ian Nicholson, J A Courinha, C A Boynard, M Pinto, “Application of phased array ultrasonic testing (PAUT) for inspection of railway axles”, The Seventh International Conference on Condition Monitoring and Machinery Failure Prevention Technologies, Straford-upon-Avon, England, June 2010.
3. http://www-civa.cea.fr [accessed 18th August 2010]
4. http://www.peakndt.com